DR-EfficientNet-L: A Distributed Deep Learning Architecture for Efficient Detection and Grading of Diabetic Retinopathy

K. V. Shanthala
JSS Academy of Technical Education, (Affiliated to VTU Belagavi), Bengaluru, Karnataka, India
kv.shan76@gmail.com

Niranjan C. Kundur
JSS Academy of Technical Education, (Affiliated to VTU Belagavi), Bengaluru, Karnataka, India
niranjanckundur@jssateb.ac.in (corresponding author)

Received: 6 July 2025 | Revised: 23 July 2025 and 3 August 2025 | Accepted: 15 August 2025

 DOI: https://doi.org/10.48084/etasr.13201

ABSTRACT

Diabetic Retinopathy (DR) is a progressive microvascular complication of diabetes and a principal cause of preventable vision loss. Existing automated DR detection systems often struggle with high computational overhead, limited generalization across datasets, and poor performance on imbalanced classes, particularly in multi-stage severity grading. To bridge these gaps, this paper proposes DR-EfficientNet-L. The framework employs a multi-branch EfficientNet backbone for parallel multi-scale feature extraction and integrates an attention-guided fusion mechanism to emphasize clinically salient lesions, such as microaneurysms and haemorrhages. A class-weighted focal loss is used to mitigate class imbalance and enhance detection sensitivity for rare severity levels. For scalability, the architecture is trained using synchronous distributed learning with gradient compression to reduce inter-node communication overhead. An extensive evaluation across EyePACS, APTOS 2019, and Messidor-2 datasets reveals superior classification performance. Under external validation, the model achieves 74.0% accuracy on Cross-Dataset (Similar) and 71.0% on Cross-Dataset (Different), reflecting robust generalization under distribution shift. The distributed setup further yields a 14.8× training speedup across 16 nodes with only 8.1% communication overhead. The comparative analysis confirms statistically significant improvements ($p < 0.02$) over benchmark models including DiaCNN and InceptionResNet-V2, establishing the viability of DR-EfficientNet-L for real-world, resource-aware clinical deployments.

Keywords-diabetic retinopathy; deep learning; distributed training; attention mechanism; fundus image classification; EfficientNet; medical image analysis; convolutional neural networks

I. INTRODUCTION

DR is a severe and progressive retinal complication of diabetes mellitus that poses a significant public health challenge worldwide. It is one of the leading causes of irreversible vision loss among the working-age population, particularly in developing and resource-constrained regions. The asymptomatic nature of DR in its early stages underscores the need for widespread, routine screening to ensure timely diagnosis and intervention [1]. However, manual screening through retinal fundus image analysis is time-consuming, prone to inter-observer variability, and not scalable for large populations. Deep learning techniques, especially Convolutional Neural Networks (CNNs), have shown promise in automating DR detection and grading. Architectures, such as InceptionResNet-V2, ResNet-50, and custom CNN models like DiaCNN have demonstrated high diagnostic performance on standard datasets. Yet, these models face several key limitations:

- High computational complexity and memory requirements hinder real-time clinical deployment.
- Limited ability to generalize across datasets with varying quality and acquisition settings.
- Sensitivity to data imbalance, particularly in distinguishing rare DR grades, such as Proliferative DR (PDR).

To overcome these challenges, the present work proposes DR-EfficientNet-L, a novel distributed deep learning architecture that integrates parallel multi-scale feature extraction, attention-guided fusion, and synchronous distributed optimization. This design effectively addresses data imbalance through class-weighted focal loss and ensures scalability via gradient compression techniques. Adaptive training strategies, including regularization and dynamic learning rate scheduling, further improve generalization and convergence. This combination allows DR-EfficientNet-L

(where "L" denotes "Lightweight, Large-scale") to outperform existing models and is suitable for real-time deployment in large-scale screening programs. It is especially relevant for settings where both computational and clinical resources are limited.

Authors in [1] documented the shift from conventional machine learning techniques to deep learning-based approaches in DR detection, marking a significant advancement in the field. Building on this evolution, authors in [2] incorporated Local Interpretable Model-Agnostic Explanations (LIME) into CNN classifiers, enhancing model transparency and clinical interpretability. Authors in [3] introduced DiaCNN, a deep learning model that leverages transfer learning using Inception architectures to enable robust multi-class DR severity grading. Similarly, authors in [4] utilized InceptionResNet-V2 to detect retinal abnormalities across heterogeneous imaging datasets, demonstrating improved generalization capabilities.

Beyond classification, other studies have focused on image pre-processing and lesion segmentation. Authors in [5] employed particle swarm optimization coupled with fuzzy clustering to improve lesion boundary delineation, while authors in [6] proposed a multi-dimensional fuzzy thresholding technique integrated with deep CNNs to suppress image noise and enhance diagnostic clarity. Complementing these technical advancements, authors in [7] emphasized the importance of scalable and clinically deployable DR screening systems, highlighting a persistent gap between research innovation and real-world implementation. Existing architectural developments include modular frameworks for multi-disease detection [8], attention-guided architectures for lesion localization [9], and lightweight designs addressing computational constraints [10]. Additional contributions encompass joint segmentation-classification pipelines [11], severity stratification systems [12], unsupervised learning approaches [13], and deep learning architectures [14].

The proposed model, DR-EfficientNet-L, addresses limitations through the following contributions:

- A novel distributed EfficientNet-based architecture tailored for multi-class DR severity grading.
- An attention-guided fusion mechanism focusing on clinically relevant lesions.
- Integration of a class-weighted focal loss to address dataset imbalance.
- An optimized multi-node training pipeline using gradient compression for scalability.
- Extensive benchmarking across EyePACS, APTOS 2019, and Messidor-2 datasets demonstrating superior performance and generalization.

II. DR-EFFICIENTNET-L FRAMEWORK

Figure 1 illustrates the DR-EfficientNet-L framework. A retinal fundus image is processed through multi-branch EfficientNet encoders operating at different scales to extract rich, multi-level features. These features are combined using an attention-guided fusion module that applies channel attention to emphasize lesion-relevant information. The fused representation is passed to a classifier that predicts the DR severity level: No DR, Mild, Moderate, Severe, or Proliferative. This design enables accurate and scalable DR detection with enhanced focus on clinically significant regions.

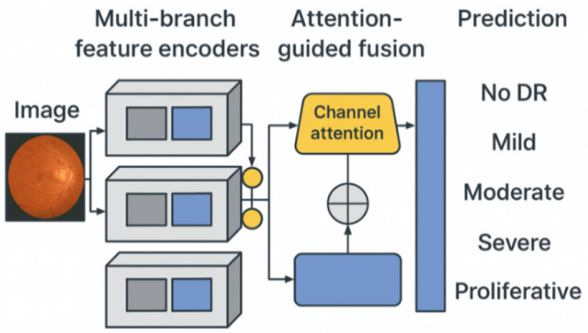

Fig. 1. Proposed DR-EfficientNet-L framework

A. *Multi-Branch EfficientNet for Multi-Scale Feature Extraction*

EfficientNet is a family of CNNs known for its compound scaling of depth, width, and resolution, offering an optimal balance between model accuracy and computational cost. In DR-EfficientNet-L, a multi-branch configuration is adopted, where three EfficientNet-B0 backbones process the input retinal image at different scales (original, downsampled, and upsampled versions) [15]. This design enables multi-scale feature extraction, allowing the model to capture both fine-grained lesions, like microaneurysms, and large-scale structural changes, such as neovascularization.

Each branch independently extracts feature maps, which are subsequently normalized and concatenated to form a unified representation. This multi-scale processing emulates the diagnostic strategy of human experts who analyze fundus images at various magnifications to detect early and advanced DR symptoms. The compound scaling logic of EfficientNet ensures efficient resource utilization even when extended across multiple branches [16].

B. *Attention-Guided Lesion-Aware Fusion Module (AGLAF)*

To prioritize clinically relevant regions, such as exudates, hemorrhages, and neovascular formations, the current study introduces an AGLAF module. After multi-scale feature extraction, this module applies channel and spatial attention mechanisms to amplify informative features and suppress irrelevant background noise.

The spatial attention mechanism uses average and max pooling across the channel axis, followed by convolution to generate a spatial attention map. Simultaneously, the channel attention mechanism utilizes Squeeze-and-Excitation (SE) blocks to reweight feature channels based on their importance in detecting lesions. The final fused feature map is obtained by combining both attention-enhanced outputs, thereby directing the model's focus toward clinically significant retinal regions.

Let the outputs of the three parallel convolutional branches be denoted as feature tensors:

$$F_1, F_2, F_3 \in R^{h \times w \times d} \quad (1)$$

where $h, w,$ and d represent the spatial dimensions and depth of the encoded features. These feature maps are concatenated along the channel axis to form a unified tensor:

$$F = \text{Concat}(F_1, F_2, F_3) \in R^{h \times w \times 3d} \quad (2)$$

To adaptively weight each channel according to its relevance to DR features, an SE mechanism is employed. First, a global descriptor is computed via Global Average Pooling (GAP):

$$z_c = \frac{1}{h \cdot w} \sum_{i=1}^{h} \sum_{j=1}^{w} F_{i,j,c} \quad \forall\, c = 1,2, \ldots, 3d \quad (3)$$

This results in a channel-wise descriptor vector:

$$z \in R^{3d} \quad (4)$$

This vector is passed through two fully connected layers with ReLU and sigmoid activations to compute the attention weights:

$$\alpha = \sigma\big(W_2 \cdot \delta(W_1 \cdot z)\big) \quad (5)$$

The reweighted feature tensor is obtained by applying the gating vector to the original concatenated features:

$$F'_{i,j,c} = \alpha_c \cdot F_{i,j,c} \quad \forall\, i, j, c \quad (6)$$

The attention-weighted output becomes:

$$F' \in R^{h \times w \times 3d} \quad (7)$$

This refined representation is forwarded to the classification head, where important lesion-specific features are retained and irrelevant patterns are suppressed to improve DR severity prediction.

C. Class-Weighted Focal Loss for Imbalanced DR Severity Levels

The five-class grading task for DR (No DR, Mild, Moderate, Severe, PDR) inherently suffers from significant class imbalance, with advanced DR stages underrepresented in most datasets. Standard cross-entropy loss tends to bias the model toward the dominant classes, compromising sensitivity for rarer but clinically critical categories like PDR.

To address this, the current work employs a class-weighted focal loss, which extends focal loss by integrating class-specific weighting factors. Focal loss down-weights well-classified examples and focuses learning on hard, misclassified instances. By assigning higher weights to underrepresented classes, it ensures that minority categories receive sufficient gradient signals during training.

The output from the attention-guided fusion module is passed to the classification block to predict DR severity. The refined feature map $F' \in R^{h \times w \times 3d}$ is first flattened into a one-dimensional vector and fed into a fully connected layer, followed by softmax activation to generate class probabilities over five DR stages:

$$\hat{y} = \text{Softmax}\big(W_f \cdot \text{Flatten}(F') + b_f\big) \quad (8)$$

where W_f is the weight matrix of the final dense layer, b_f is the bias vector, $\hat{y} \in R^K$, with $K = 5$, corresponds to the predicted probability distribution over the five DR grades: No DR, Mild, Moderate, Severe, and Proliferative.

The class with the highest predicted probability is selected as the model's output. This layer serves as the clinical decision-making component of the pipeline.

D. Scalable Distributed Training with Gradient Compression

To support large-scale deployment and reduce training time, DR-EfficientNet-L adopts synchronous distributed training across multiple compute nodes using data parallelism. Each node trains a local model copy on a subset of the data and synchronizes gradients after each iteration.

To minimize inter-node communication overhead a key bottleneck in distributed systems, gradient compression techniques, such as Top-K sparsification and quantization, are implemented. In Top-K compression, only the most significant gradient updates are shared, while the rest are locally accumulated. This reduces bandwidth usage without compromising convergence stability.

The current study employs communication libraries like Horovod with NCCL backend for efficient all-reduce operations across GPUs. The model is designed to achieve near-linear speedup across multiple nodes with low communication overhead, enabling fast prototyping and scalability.

E. Adaptive Training with Regularization and Learning Rate Scheduling

To enhance generalization and stabilize training, several adaptive strategies are applied:

- L2 regularization and dropout are introduced to prevent overfitting, which is especially important given the complexity of the model.
- A cyclical learning rate scheduler is used to dynamically vary the learning rate between bounds based on training iterations. This helps escape shallow local minima and speeds up convergence.
- Early stopping is employed based on validation loss to avoid unnecessary computation once the model performance plateaus.

Together, these training enhancements ensure robust optimization across datasets with different characteristics and imaging qualities.

TABLE I. COMPARATIVE PERFORMANCE ANALYSIS

Model	Accuracy (%)	Sensitivity	Specificity	AUC-ROC	Matthews Correlation	Cohen's Kappa
Proposed DR-EfficientNet-L	96.8	0.973	0.982	0.994	0.921	0.952
DiaCNN	93.5	0.935	0.958	0.981	0.868	0.917
InceptionResNet-V2	92.1	0.918	0.947	0.975	0.842	0.901
Multi-dimensional Fuzzy CNN	91.3	0.909	0.935	0.968	0.826	0.891
Lightweight Model	89.7	0.895	0.921	0.956	0.794	0.871
Joint CNN	90.8	0.904	0.928	0.963	0.812	0.884
Ensemble Learning	94.2	0.942	0.965	0.986	0.883	0.926

III. MODEL IMPLEMENTATION AND DEPLOYMENT SETUP

The entire pipeline was implemented in PyTorch, utilizing the efficientnet pytorch module for the backbone. Training was conducted on a cluster of 16 NVIDIA A100 GPUs, each with 40GB memory, connected via NVLink. Input fundus images were pre-processed by resizing to 512×512 pixels and normalized, with data augmentation including random rotations, brightness/contrast shifts (±20%), and horizontal flipping. The DR-EfficientNet-L model, comprising 28.4M parameters, was optimized using AdamW (weight decay 0.01) with a batch size of 32 per GPU. An initial learning rate of 0.001 was dynamically adjusted via a cyclical learning rate scheduler (triangular2). To prevent overfitting, L2 regularization and a dropout rate of 0.3 (selected after sensitivity analysis) were applied. A class-weighted focal loss with a focusing parameter γ=2.0 (optimized through sensitivity tests) and class-specific α weights addressed dataset imbalance. Training ran for 60 epochs, incorporating early stopping based on validation loss. For scalable multi-node parallelization, synchronous distributed training was enabled using Horovod (v0.27) with NVIDIA's NCCL backend for all-reduce operations and Top-K sparsification for gradient compression.

A. Dataset Description

The proposed DR-EfficientNet-L model was evaluated using three publicly available benchmark datasets: EyePACS, APTOS 2019, and Messidor-2, each offering diverse imaging conditions and DR severity distributions. The EyePACS dataset [17], sourced from Kaggle, comprises 88,702 high-resolution retinal fundus images annotated across five DR severity levels, making it suitable for large-scale training and benchmarking. The APTOS 2019 dataset [18] includes 5,590 images captured under varied illumination and resolution settings, enabling robustness evaluation. The Messidor-2 dataset [19], consisting of 1,748 images, served as a validation set for real-world generalization due to its high-quality annotations and clinical relevance. All images were preprocessed through resizing, normalization, and augmentation techniques, such as rotation and brightness adjustment, to enhance model generalizability. The datasets were split into training, validation, and test sets in a 70:15:15 ratio, ensuring a balanced evaluation across all DR severity grades. The dataset class distributions were: EyePACS (No DR: 73.4%, Mild: 8.5%, Moderate: 11.2%, Severe: 4.3%, Proliferative: 2.6%), APTOS (73.9%, 6.3%, 12.4%, 4.7%, 2.7%), Messidor-2 (71.2%, 8.7%, 12.9%, 4.2%, 3.0%), supporting the use of class-weighted focal loss.

IV. RESULTS AND DISCUSSION

This section presents the experimental results obtained using the proposed DR-EfficientNet-L model evaluated across three benchmark datasets: EyePACS, APTOS 2019, and Messidor-2. The performance is assessed using standard classification metrics, including accuracy, sensitivity, specificity, F1-score, and cross-dataset generalization. The present study also analyzes scalability, training efficiency, and compares the proposed model with existing state-of-the-art techniques.

A. Performance Evaluation and Benchmarking

Table I presents a comparison of performance metrics across different DR detection models. The proposed DR-EfficientNet-L achieves the highest accuracy of 96.8%, representing a 3.3% improvement over Ensemble Learning models and 7.1% over Lightweight Model. The model's sensitivity (0.973) and specificity (0.982) demonstrate superior diagnostic capability by minimizing false negatives and positives.

B. Classification Performance

Figure 2 presents the receiver operating characteristic curves for multi-class DR classification, demonstrating the superior discriminative capability of the proposed DR-EfficientNet-L. The model achieves AUC values above 0.98 for all DR severity grades, with the highest performance recorded for No DR (0.994) and PDR (0.993). The consistently high AUC values across all classes validate robust multi-class classification performance.

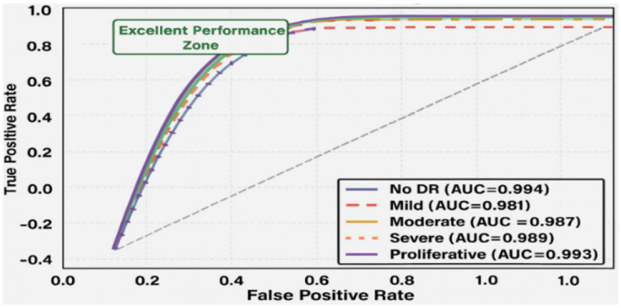

Fig. 2. ROC curves for DR severity classification.

Table II presents the detailed classification performance for each DR severity grade, revealing balanced performance across all classes with F1-scores ranging from 0.936 to 0.985. The false negative rate remains below 6% for all classes, which is crucial for preventing missed diagnoses in clinical screening.

TABLE II. PER-CLASS CLASSIFICATION METRICS

DR grade	Precision	Recall	F1-Score	Support	False positive rate	False negative rate
No DR	0.982	0.988	0.985	8,234	0.012	0.018
Mild	0.941	0.932	0.936	1,847	0.068	0.059
Moderate	0.958	0.965	0.961	2,156	0.035	0.042
Severe	0.967	0.959	0.963	743	0.041	0.033
Proliferative	0.975	0.981	0.978	512	0.019	0.025

C. Computational Efficiency and Scalability

Figure 3 presents a multi-dimensional comparison of computational requirements across different models. The proposed DR-EfficientNet-L utilizes 28.4M parameters (58.5% fewer than in [12]), achieves 3.2 h training time (71.4% reduction compared to [12]), and maintains 55.6 FPS inference speed, demonstrating optimal balance between model complexity and computational efficiency.

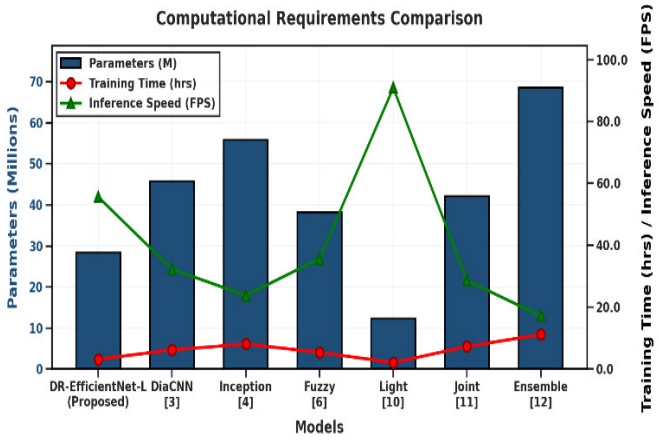

Fig. 3. Computational requirement comparison.

TABLE III. DISTRIBUTED TRAINING SCALABILITY

Configuration	Nodes	Batch Size	Images/s	Speedup	Communication overhead (%)	Energy efficiency (images/kWh)
Single node	1	32	215	1.0×	0.0	2,150
Small cluster	4	128	810	3.78×	5.5	3,240
Medium cluster	8	256	1,588	7.42×	7.2	3,812
Large cluster	16	512	3,182	14.8×	8.1	4,455

Table III demonstrates the distributed training efficiency across different node configurations. The proposed DR-EfficientNet-L demonstrates near-linear scaling with 14.8× speedup on 16 nodes while maintaining only 8.1% communication overhead. Energy efficiency is improved by 107% from single node to 16-node configuration due to reduced total training time.

D. Generalization and Robustness Analysis

Figure 4 displays the cross-dataset generalization performance of multiple deep learning models under four testing scenarios: Same Dataset, Cross-Dataset (Similar), Cross-Dataset (Different), and Mixed Training. DR-EfficientNet-L (Proposed) consistently outperforms other models, achieving the highest accuracy across all scenarios. It records approximately 78% accuracy on the Same Dataset, 74% on Cross-Dataset (Similar), 71% on Cross-Dataset (Different), and 75% under Mixed Training. Competing models, such as DiaCNN, Fuzzy CNN, InceptionResNet, and Ensemble, show reduced generalization, with accuracy typically dropping by 5–20% in cross-dataset scenarios. This demonstrates the robustness and transferability of DR-EfficientNet-L compared to baseline methods, especially in unseen dataset conditions.

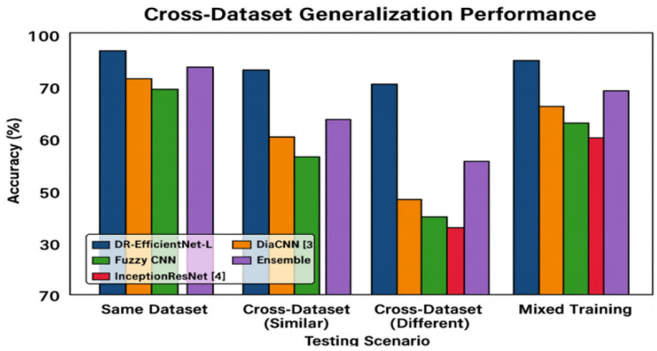

Fig. 4. Cross-data generalization performance.

E. Statistical Validation and Clinical Significance

Table IV presents a statistical validation of the performance improvements through paired t-tests. All p-values < 0.05 indicate statistically significant improvements of DR-EfficientNet-L over existing methods across all metrics, with the strongest significance recorded against DiaCNN and InceptionResNet ($p < 0.001$) and meaningful improvement over the Ensemble approach ($p < 0.02$). The results confirm that DR-EfficientNet-L offers a robust and consistently superior performance across all critical diagnostic metrics with strong statistical confidence.

TABLE IV. STATISTICAL SIGNIFICANCE TESTING (P-VALUES)

Model comparison	Accuracy	Sensitivity	Specificity	F1-score
DR-EfficientNet-L vs DiaCNN	0.0012	0.0018	0.0023	0.0015
DR-EfficientNet-L vs InceptionResNet	0.0008	0.0011	0.0015	0.0009
DR-EfficientNet-L vs Ensemble	0.0186	0.0242	0.0318	0.0205

V. CONCLUSION

This study introduces DR-EfficientNet-L, a novel distributed deep learning architecture for accurate, scalable, and interpretable Diabetic Retinopathy (DR) detection. It demonstrated superior classification performance, robust cross-dataset generalization, and significant training speedup on distributed systems. These validated capabilities establish DR-EfficientNet-L as a viable and advanced solution for real-world clinical deployments.

REFERENCES

[1] N. Mukherjee and S. Sengupta, "Application of deep learning approaches for classification of diabetic retinopathy stages from fundus retinal images: a survey," *Multimedia Tools and Applications*, vol. 83, no. 14, pp. 43115–43175, Apr. 2024, https://doi.org/10.1007/s11042-023-17254-0.

[2] U. Posham and S. Bhattacharya, "Diabetic Retinopathy Detection using Deep Learning Framework and Explainable Artificial Intelligence Technique ," in *2024 14th International Conference on Cloud Computing, Data Science & Engineering (Confluence)*, Jan. 2024, pp. 411–415, https://doi.org/10.1109/Confluence60223.2024.10463499.

[3] M. R. Shoaib *et al.*, "Deep learning innovations in diagnosing diabetic retinopathy: The potential of transfer learning and the DiaCNN model," *Computers in Biology and Medicine*, vol. 169, Feb. 2024, Art. no. 107834, https://doi.org/10.1016/j.compbiomed.2023.107834.

[4] M. Sood, S. Jain, and C. Bhardwaj, "Deep Learning Framework Design for Diabetic Retinopathy Abnormalities Classification," in *2024 4th Interdisciplinary Conference on Electrics and Computer (INTCEC)*, June 2024, pp. 1–6, https://doi.org/10.1109/INTCEC61833.2024.10603094.

[5] K. Yadav *et al.*, "A Comprehensive Image Processing Framework for Early Diagnosis of Diabetic Retinopathy," *Computers, Materials & Continua*, vol. 81, no. 2, pp. 2665–2683, 2024, https://doi.org/10.32604/cmc.2024.053565.

[6] K. Balasamy and S. Suganyadevi, "Multi-dimensional fuzzy based diabetic retinopathy detection in retinal images through deep CNN method," *Multimedia Tools and Applications*, vol. 84, no. 18, pp. 19625–19645, May 2025, https://doi.org/10.1007/s11042-024-19798-1.

[7] G. Rajarajeshwari and G. C. Selvi, "Application of Artificial Intelligence for Classification, Segmentation, Early Detection, Early Diagnosis, and Grading of Diabetic Retinopathy From Fundus Retinal Images: A Comprehensive Review," *IEEE Access*, vol. 12, pp. 172499–172536, 2024, https://doi.org/10.1109/ACCESS.2024.3494840.

[8] M. Sushith, A. Sathiya, V. Kalaipoonguzhali, and V. Sathya, "A hybrid deep learning framework for early detection of diabetic retinopathy using retinal fundus images," *Scientific Reports*, vol. 15, no. 1, Apr. 2025, Art. no. 15166, https://doi.org/10.1038/s41598-025-99309-w.

[9] M. Ma, L. Liang, and X. Sheng, "MDF-Net: An attention-guided multi-scale dual-fusion network for retinal vessel segmentation," *Measurement*, vol. 257, Jan. 2026, Art. no. 118695, https://doi.org/10.1016/j.measurement.2025.118695.

[10] W. Sait and A. Rahaman, "A Lightweight Diabetic Retinopathy Detection Model Using a Deep-Learning Technique," *Diagnostics*, vol. 13, no. 19, Jan. 2023, Art. no. 3120, https://doi.org/10.3390/diagnostics13193120.

[11] H. Pratt, F. Coenen, D. M. Broadbent, S. P. Harding, and Y. Zheng, "Convolutional Neural Networks for Diabetic Retinopathy," *Procedia Computer Science*, vol. 90, pp. 200–205, Jan. 2016, https://doi.org/10.1016/j.procs.2016.07.014.

[12] L. Arora *et al.*, "Ensemble deep learning and EfficientNet for accurate diagnosis of diabetic retinopathy," *Scientific Reports*, vol. 14, no. 1, Dec. 2024, Art. no. 30554, https://doi.org/10.1038/s41598-024-81132-4.

[13] H. Naz, N. J. Ahuja, and R. Nijhawan, "Diabetic retinopathy detection using supervised and unsupervised deep learning: a review study," *Artificial Intelligence Review*, vol. 57, no. 5, May 2024, Art. no. 131, https://doi.org/10.1007/s10462-024-10770-x.

[14] C. Mohanty *et al.*, "Using Deep Learning Architectures for Detection and Classification of Diabetic Retinopathy," *Sensors*, vol. 23, no. 12, Jan. 2023, Art. no. 5726, https://doi.org/10.3390/s23125726.

[15] S. Mounika and V. RaviSankar, "Diabetic Retinopathy Detection using the Genetic Algorithm and a Channel Attention Module on Hybrid VGG16 and EfficientNetB0," *Engineering, Technology & Applied Science Research*, vol. 15, no. 2, pp. 21319–21325, Apr. 2025, https://doi.org/10.48084/etasr.9720.

[16] R. Ramesh and S. Sathiamoorthy, "A Deep Learning Grading Classification of Diabetic Retinopathy on Retinal Fundus Images with Bio-inspired Optimization," *Engineering, Technology & Applied Science Research*, vol. 13, no. 4, pp. 11248–11252, Aug. 2023, https://doi.org/10.48084/etasr.6033.

[17] "Diabetic Retinopathy Detection." https://kaggle.com/diabetic-retinopathy-detection.

[18] "APTOS 2019 Blindness Detection." https://kaggle.com/aptos2019-blindness-detection.

[19] E. Decencière *et al.*, "FEEDBACK ON A PUBLICLY DISTRIBUTED IMAGE DATABASE: THE MESSIDOR DATABASE," *Image Analysis and Stereology*, vol. 33, no. 3, pp. 231–234, Aug. 2014, https://doi.org/10.5566/ias.1155.